Evaluation of ^{111}In-labeled Anginex as Potential SPECT Tracer for Imaging of Tumor Angiogenesis

TIEMEN R. VAN MOURIK[1], TILMAN LÄPPCHEN[2], RAFFAELLA ROSSIN[2,3], JUDY R. VAN BEIJNUM[4], JOHN R. MACDONALD[5], KEVIN H. MAYO[6], ARJAN W. GRIFFIOEN[4], KLAAS NICOLAY[1] and HOLGER GRÜLL[1,2]

[1]*Department of Biomedical Engineering, Eindhoven University of Technology, Eindhoven, the Netherlands;*
[2]*Oncology Solutions, Philips Research, Eindhoven, the Netherlands;*
[3]*Tagworks Pharmaceuticals, Eindhoven, the Netherlands;*
[4]*Angiogenesis Laboratory, Department of Medical Oncology, VU University Medical Center, Amsterdam, the Netherlands;*
[5]*PepTx, Inc., Excelsior, Minnesota, MN, U.S.A.;*
[6]*Department of Biochemistry, University of Minnesota, Minneapolis, MN, U.S.A.*

Abstract. *Angiogenesis is a prerequisite for solid tumors to grow and metastasize, providing oxygen and nutrients to the tumor site. The protein galectin-1 has been identified to be overexpressed on tumor vasculature and represents an interesting target for anti-angiogenic therapy, as well as in molecular imaging. Therefore, the galectin-1-binding peptide Anginex was modified for radiolabeling using ^{111}In. In vitro, ^{111}In-Ax showed significantly more binding to galectin-1-positive EC-RF24 and MDA-MB-231-LITG cells than to galectin-1-negative LS174T cells and association with EC-RF24 cells was reduced in the presence of excess native Anginex. However, ex vivo biodistribution profiles showed little tumor uptake of ^{111}In-Ax and extensive accumulation in non-target organs. Although this study shows the ease of modification of the therapeutic peptide Anginex and favorable characteristics in vitro, in vivo assessment of the tracer revealed negligible tumor targeting. Hence, the strategy we employed lends little support for successful non-invasive imaging of tumor angiogenesis using this peptide.*

Tumor angiogenesis, the formation of new blood vessels in neoplastic tissues, is one of the hallmarks in cancer development (1, 2). Developing tumors trigger angiogenesis for a sustained nutrient and oxygen supply in order to grow beyond sizes of 1-2 mm^3 (3-5). Due to its importance in tumor development, angiogenesis presents a valuable target in drug treatment as well as in molecular imaging approaches for early cancer detection (6, 7). During recent years, a plethora of angiogenesis-related target molecules have been studied (8, 9). Particularly suited are targets that are overexpressed on endothelial cells (ECs) lining the luminal side of angiogenic blood vessels and are furthermore only overexpressed on ECs in tumors and not in healthy tissue vasculature (10). In this context, galectin-1 has been identified as a potential target for EC-directed anti-angiogenic therapy and targeted imaging applications for early cancer diagnostics (11, 12). Hence, galectin-1 may present a more general target compared to specific cell surface markers that are overexpressed on cancer cells, which may strongly depend on the particular type of cancer. Furthermore, due to its prominent role in cell adhesion, migration and proliferation, galectin-1 has been shown to be a prognostic biomarker as expression levels are linked to a greater resistance in therapeutics and thus a poor prognosis (11-16).

Recently, the designed, β-sheet forming 33-mer peptide Anginex was demonstrated to bind galectin-1 and to possess anti-angiogenic properties (17-21). The positively-charged, amphipathic peptide has been reported to selectively bind to galectin-1 with a K_d in the μM range (11). Studies indicated that Anginex specifically blocks the adhesion and migration of angiogenically activated ECs, but not dormant or pre-existing blood vessels, resulting in an inhibition of EC growth with a half-maximal inhibitory effect at ~1.5 μM (11, 12, 17, 19, 22). Due to its anti-angiogenic effect *in vitro* and *in vivo*, Anginex has been studied as a possible therapeutic agent in oncology (17, 22). Although galectin-1 provides a

Correspondence to: Professor Dr. Holger Grüll, Eindhoven University of Technology, Dept. of Biomedical Engineering, High Tech Campus 11 (p2.61), 5656 AE Eindhoven, the Netherlands. Tel: +31 0612932309, Fax: +31 402743350, e-mail: h.gruell@tue.nl

Key Words: Anginex, tumor angiogenesis, galectin-1, cancer, indium-111.

suitable target for anti-angiogenic therapy, galectin-1-targeted imaging approaches for cancer detection or potential imaging of anti-angiogenic therapy remain limited. Using Anginex as an affinity ligand for galectin-1, Brandwijk *et al*. applied Anginex-coated, fluorescently labeled paramagnetic liposomes to human umbilical vein endothelial cell (HUVEC) cultures, showing binding 3 h post-incubation and internalization of the Anginex-conjugated liposomes in cell pellets by magnetic resonance imaging (MRI) measurements (23). In a dual targeting MRI approach, Kluza *et al*. employed liposomes modified with both Anginex and Arg-Gly-Asp (RGD) peptides for, respectively, galectin-1 and $a_v\beta_3$ targeting *in vitro* and *in vivo* (24, 25). This strategy provided a two-fold elevated uptake of the dual targeted liposomes over single targeted agents, showing a synergistic effect of targeting two cell surface located markers and providing a more reliable MRI readout of the angiogenic activity. Furthermore, Apana and co-workers developed ^{18}F-labeled Anginex, allowing static positron emission tomography (PET) visualization of a BN myeloma tumor/bone graft 2 h post *i.p*. injection in SCID-rab mice and dynamic PET in FSall tumor-bearing mice displayed a positive tumor-to-muscle ratio as early as a few minutes post *i.p*. tracer injection (26).

We hypothesized that by modifying the therapeutic Anginex peptide with a 1,4,7,10-tetra-azacyclododecane-1,4,7,10-tetra-acetic acid (DOTA) moiety (Ax-DOTA, Figure 1A) for labeling with a suitable radionuclide for nuclear imaging [*e.g*. single photon emission computed tomography (SPECT)], we would obtain a radiotracer that allows imaging of angiogenesis by targeting galectin-1 overexpressed on activated ECs. Due to the elongated half-life of ^{111}In in comparison to ^{18}F, we can perform imaging experiments after prolonged circulation times and visualize the *in vivo* fate of the therapeutic peptide Anginex. Furthermore, the DOTA moiety has the possibility for radiolabeling with other radioisotopes such as ^{177}Lu or ^{90}Y, thus providing the option for targeted radiotherapy of tumor growth. Therefore, we developed an ^{111}In-labeled Anginex tracer (^{111}In-Ax) for SPECT imaging and tested it *in vitro* as well as *in vivo*. As a model for tumor ECs *in vitro* we used EC-RF24 cells, which overexpress galectin-1 in the presence of angiogenic growth factors (27). In order to further investigate galectin-1 expression levels in cancer cells, we used the galectin-1 expressing MDA-MB-231-LITG breast cancer cell line in comparison to the LS174T colon cancer cell line having a low expression level of galectin-1 (28). While a clear difference in tracer uptake between these cell lines was expected *in vitro*, we did not expect *in vivo* studies to demonstrate a large variation between them, provided the tracer primarily targeted galectin-1 on ECs lining the tumor vasculature. However, the presence of tumor-derived galectin-1 in the tumor ECs could induce an elevated uptake in the galectin-1 expressing MDA-MB-231-LITG tumor bearing mice (15).

In our study, we employed negative control βpep28-DOTA (Figure 1B), a peptide identical in length and folded structure but whose galectin-1-binding properties are significantly reduced (17, 19). ^{111}In-Ax was characterized *in vitro* employing cell-based binding and competition assays, followed by further *in vivo* evaluation of ^{111}In-Ax in terms of blood clearance, pharmacokinetics, and tumor targeting in nude mice bearing MDA-MB-231-LITG and LS174T human tumor xenografts (28).

Materials and Methods

Peptide tracer synthesis. All reagents were obtained from Sigma-Aldrich (Zwijndrecht, the Netherlands) in the highest available quality and were used as received unless stated otherwise. 2,2',2''-(10-(2-((2-(2,5-Dioxo-2,5-dihydro-1*H*-pyrrol-1-yl)ethyl)amino)-2-oxoethyl)-1,4,7,10-tetra-azacyclododecane-1,4,7-triyl)triacetic acid (maleimido-mono-amide-DOTA) was purchased from Macrocyclics (Dallas, TX, USA). Peptides (Anginex, C-Cys-Anginex, C-Cys-βpep28) were provided by Kevin Mayo (University of Minnesota, MN, USA). The peptides (C-Cys-Anginex: H_2N-ANIKLSVQ MKLFKRHLKWKIIVKLNDGRELSLDC-COOH; C-Cys-βpep28: H_2N-SIQDLNVSMKLFRKQAKWKVIVKLNDGR ELSLDC-COOH) were modified with maleimide-mono-amide-DOTA by incubating a 1 mg/ml aqueous solution of the peptide with a 1.1 molar excess of the activated DOTA overnight at room temperature. After conjugation, no unmodified peptide was present and the excess of maleimide-mono-amide-DOTA was removed by preparative reversed-phase high-performance liquid chromatography (HPLC). The DOTA-conjugated peptides Ax-DOTA and βpep28-DOTA were purified using preparative HPLC on a Zorbax C18 column (21.5×150 mm, 5 μm particle size; Agilent Technologies, Santa Clara, CA, USA) equipped with a pre-column and were eluted with water (solvent A) and acetonitrile (ACN; solvent B) containing 0.1% trifluoroacetic acid at a 10 ml/min flow (gradient: 5 min 0% to 30% solvent B, 15 min 30% to 60% solvent B, 2 min 60% to 95% solvent B, 5 min 95% solvent B). High-resolution mass spectra were recorded on an Agilent electrospray ionization-time-of-flight mass spectrometer, measuring in the positive ion mode.

Radiolabeling. [^{111}In]Indium chloride ($^{111}InCl_3$) solutions were obtained from Perkin-Elmer (Waltham, MA, USA) and Mallinckrodt Pharmaceuticals (Zaltbommel, the Netherlands). The buffers used for radiolabeling were treated with Chelex-100 resin (Bio-Rad, Hercules, CA, USA) before use. Ax-DOTA and βpep28-DOTA were radiolabeled with ^{111}In in ammonium acetate buffer (0.2 M, pH 5.5) at 90˚C for 5 min, labeling 1 μg of peptide to a specific activity of 1 MBq/μg in a volume of 50 μl. Subsequently, the loosely bound ^{111}In was challenged with diethylene triaminepenta-acetic acid (DTPA; 1 eq. to the peptide). Radiochemical yields were determined by instant thin layer chromatography (iTLC) using silica gel strips eluted with 200 mM ethylene diaminetetra-acetic acid (EDTA) in saline (^{111}In-labeled peptide: Rf=0.0; ^{111}In: Rf=0.9) and radiochemical purity was determined with HPLC. Radio-TLC was performed on iTLC-SG strips (Biodex Medical Systems, Shirley, NY, USA), which were analyzed on a FLA-7000 phosphorimager (FujiFilm, Tokyo, Japan) using AIDA software (Raytest,

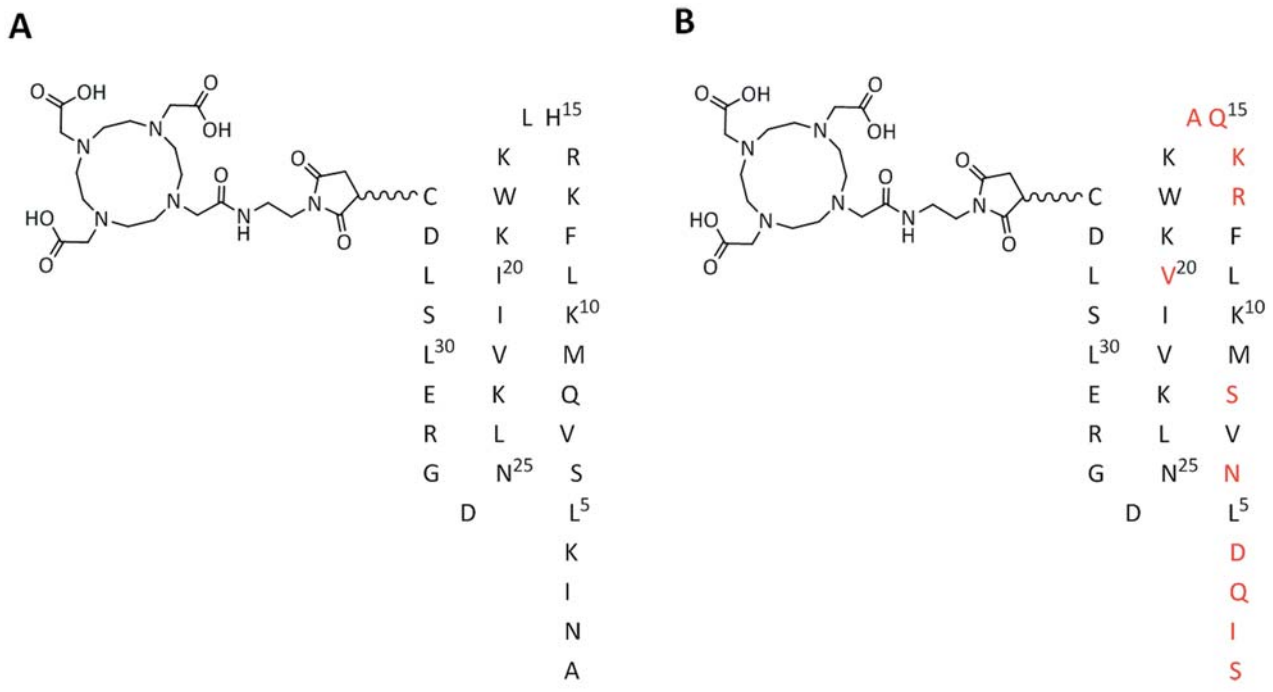

Figure 1. *One-letter code amino acid denotations of the folded β-sheets of 1,4,7,10-tetraazacyclododecane-1,4,7,10-tetra-acetic acid (DOTA)-modified C-Cys-Anginex (Ax-DOTA) (A) and the negative control DOTA-modified C-Cys-βpep28 (B). The deviating parts of the βpep28 sequence are highlighted in red.*

Straubenhardt, Germany). Analytical reversed-phase HPLC was performed on an Agilent 1100 system equipped with UV and radioactive detectors (Raytest). The analytes were injected on a Zorbax Eclipse C18 XBD-column (4.6×150 mm, 5 μm particle size; Agilent Technologies) equipped with a pre-column and were eluted at 1 ml/min flow using solvents A and B described above (gradient: 3 min 5% solvent B, 15 min 5% to 60% solvent B, 1 min 50% to 100% solvent B, 2 min 100% solvent B). The radiolabeled peptides ^{111}In-Ax and ^{111}In-βpep28 showed greater than 95% radiochemical purity and were used without further purification.

In vitro studies. Cells were provided by Arjan Griffioen (EC-RF24; VU Medical Center, Amsterdam, the Netherlands), a kind gift of Clemens Löwik (MDA-MB-231-LITG; Leiden University Medical Center, Leiden, the Netherlands) or purchased from the ATCC (LS174T; Manassas, VA, USA). Cells were cultured in media obtained from Gibco (Medium 199, Dulbecco's minimal essential medium and Eagle's minimal essential medium, respectively; Bleiswijk, the Netherlands), supplemented with 10% heat inactivated fetal bovine serum, 1% penicillin (100 U/ml), 1% streptomycin (100 μg/ml) and 1% L-glutamine (200 mM). EC-RF24 cells were cultured with an additional 18 ng/ml basic fibroblast growth factor (Sigma Aldrich) to induce galectin-1 overexpression. Cells were used when near-confluent and prior to incubation, were harvested using 0.25% w/v trypsin-EDTA (Gibco) and seeded in 24-well plates at a concentration of 20,000 cells per well in culture medium and allowed to adhere for 16 h. Cells were then incubated in fresh culture medium supplemented with ^{111}In-Ax or ^{111}In-βpep28 alone (10 nM), or with ^{111}In-Ax in combination with either a 1000-fold excess of native Anginex or C-Cys-βpep28 (βpep28). At different time points (longitudinal assays: 0.5, 1, 2, 4, and 24 h; cross-sectional assays: 4 h), cells were washed with Dulbecco's phosphate-buffered saline (PBS) and collected using a 0.5% sodium dodecyl sulfate solution for measurements in a γ-counter (Wizard 1480 γ-counter, energy window 100-510 keV; Perkin-Elmer). Protein quantification for normalization was obtained using a BCA Protein Assay Kit (Thermo Fisher Scientific, Pierce, Rockford, IL, USA) and data are expressed as the mean percentage incubated dose per microgram of protein (%ID/μg).

In vivo studies. All animal procedures were approved by the Maastricht University Ethical Review Committee (DEC-UM 2011-163) and were performed according to the Dutch national law "Wet op de Dierproeven" (Staatsblad 1985, 336) and the Institutional Animal Care Committee guidelines. Female Balb/c nude mice (8 weeks old) were obtained from Charles River (Burlington, MA, USA) and were housed in an enriched environment under standard conditions: 21-23˚C, 50-60% humidity and 12 h light-dark cycles. Food and water were freely available. Tumors were grown on the hind leg of the mice by a subcutaneous/intramuscular injection of MDA-MB-231-LITG or LS174T cells (3×10^6 cells in 100 μl sterile PBS, pH 7.4, n=3 per group). Tumor size was monitored twice a week, and animals were used for tracer studies 2-6 weeks post tumor cell injection (tumor size 50-300 mm^3).

In vivo blood kinetics and ex vivo biodistribution. *In vivo* blood kinetic measurements and *ex vivo* biodistribution profiles were obtained in 12 MDA-MB-231-LITG and LS174T tumor-bearing mice. Following

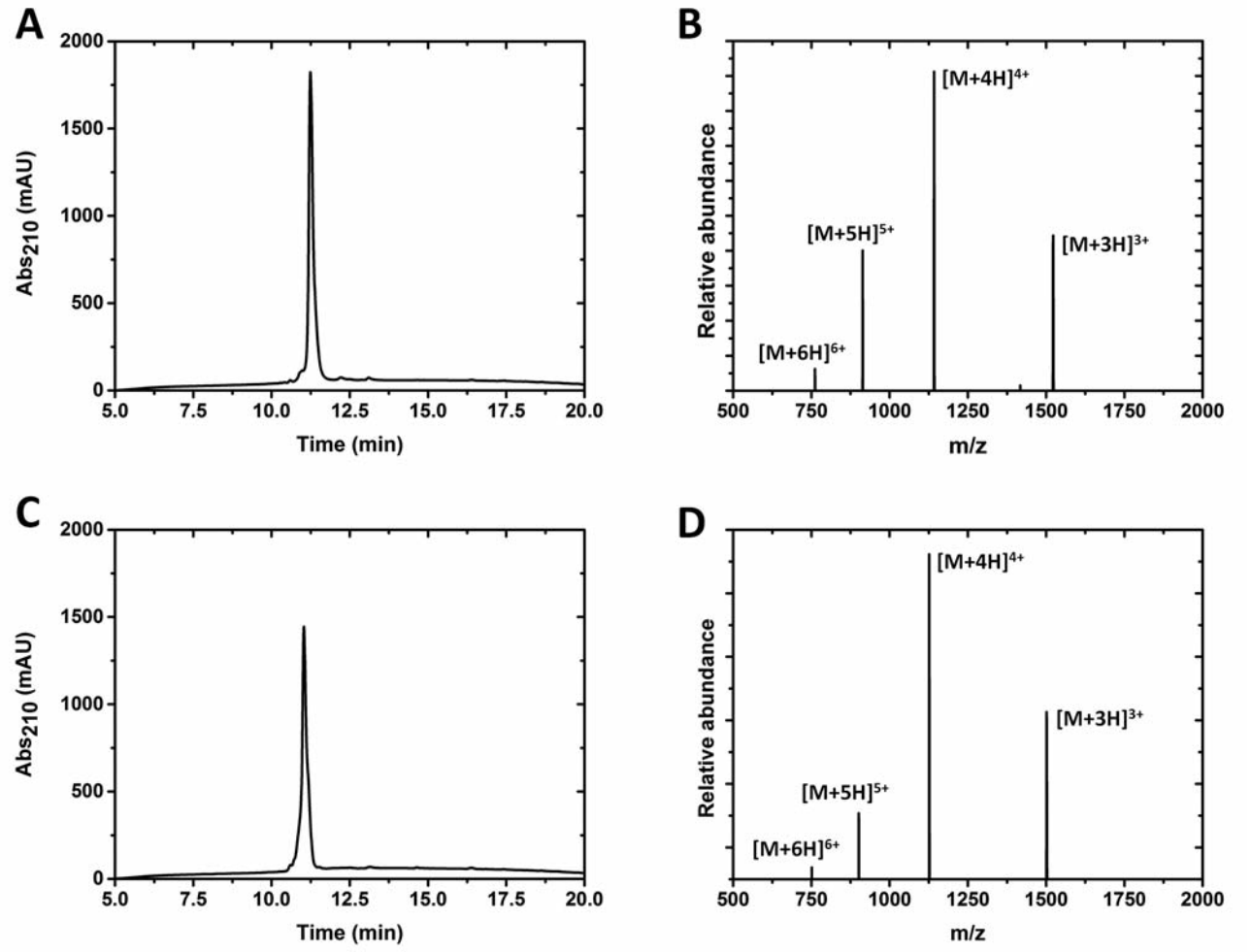

Figure 2. *Liquid chromatography-mass spectrometry chromatograms and corresponding mass spectra of Anginex-1,4,7,10-tetraazacyclododecane-1,4,7,10-tetraacetic acid (DOTA) (A, B) and βpep28-DOTA (C, D).*

intravenous injection with ^{111}In-Ax [50 μg/kg bodyweight (b.w.), 100 μl, ~1 MBq/μg or 5 μg/kg b.w., 100 μl, ~1 MBq/μg, n=3 per tumor model], blood samples (20 μl) were taken at various time points (MDA-MB-231-LITG: 2, 5, 10, 45, 120 and 240 min; LS174T: 2, 5, 10, 30, 60 and 180 min). Mice were anesthetized and euthanized by cervical dislocation either 3 h (5 μg/kg b.w., both tumor models), 6 h (50 μg/kg b.w., LS174T) or 24 h (50 μg/kg b.w., MDA-MB-231-LITG) post tracer injection, and a final blood sample was obtained by heart puncture. The tumors and other tissues were harvested, blotted dry and weighed, and the radioactivity was measured using a γ-counter, along with standards to determine the mean percentage injected dose per gram tissue (%ID/g) and the mean percentage injected dose (%ID). Urine samples were analyzed with analytical HPLC. The probe concentration at t=0 (C_0) was calculated by fitting the blood kinetic curves to a two-phase exponential decay function $y=A_1 \times \exp(-x/t_1) + A_2 \times \exp(-x/t_2) + y_0$ using Origin software (OriginLab, Northampton, MA, USA), subsequently deriving the half-lives ($t_{1/2,\alpha}=t_1 \times \ln 2$, $t_{1/2,\beta}=t_2 \times \ln 2$). The volume of distribution (V_D) per mouse was calculated as V_D=dose/(b.w. × C_0) (l/kg).

Data analysis and statistics. Data represent the mean value±standard deviation (SD). For differences between two groups, data sets were compared using unpaired two-sided *t*-tests (not assuming equal variances). *p*-Values less than 0.05 were considered significant. Data analysis was performed with Origin 9.0.0 SR2.

Results

Synthesis and radiolabeling. Selective, C-terminal conjugation of the DOTA moiety to the peptides was achieved by maleimide-thiol conjugation chemistry employing C-Cys-modified versions of the galectin-1 binding peptide Anginex and negative control βpep28 (Figure 1). LC-MS analysis of the purified peptides after preparative HPLC revealed greater than 95% purity (UV), while the identities of Ax-DOTA and βpep28-DOTA were confirmed by mass spectra, which showed values in agreement with the expected molecular mass (Ax-DOTA:

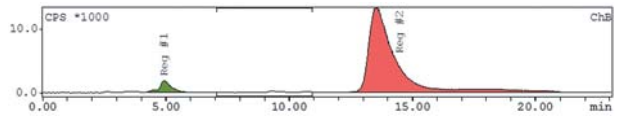

Figure 3. *High-performance liquid chromatography radio-trace of ^{111}In-Ax, showing free $^{111}InCl_3$ (Reg #1, 4.73%) and ^{111}In-labeled Anginex (^{111}In-Ax, Reg #2, 95.27%). UV absorbance at 212 nm is not shown because the trace amounts of peptide are not visible in the chromatogram.*

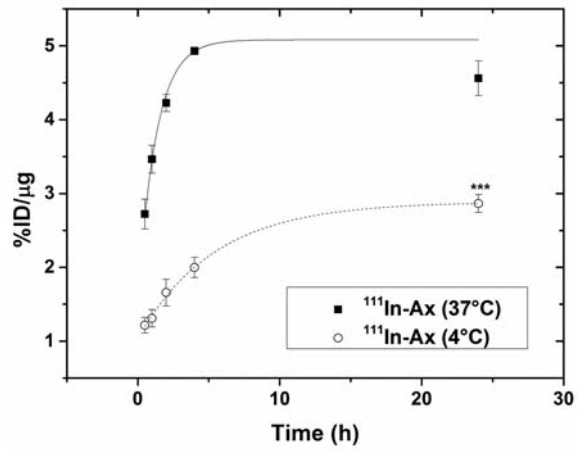

Figure 4. *Time course for binding of ^{111}In-Ax (10 nM) at 4˚C and 37˚C. Data are presented as %ID/µg of protein ± SD (n=5) and fitted with an exponential function. ***p<0.001 vs. ^{111}In-Ax at 37˚C.*

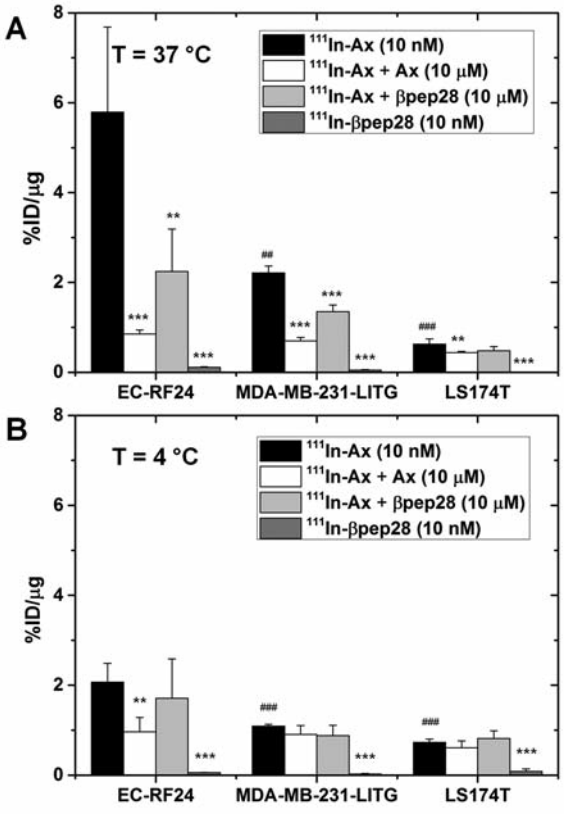

Figure 5. *Binding of ^{111}In-Ax (10 nM) with and without native Anginex (10 µM) or βpep28 (10 µM) and ^{111}In-βpep28 (10 nM) to EC-RF24, MDA-MB-231-LITG or LS174T cell cultures at 37˚C (A) and 4˚C (B) after 4 h incubation. Data are presented as %ID/µg of protein±SD (n=5). ##p<0.01, ###p<0.001 vs. ^{111}In-Ax/EC-RF24; **p<0.01, ***p<0.001 vs. ^{111}In-Ax within the same cell type.*

MW 4562.5 Da, Figure 2A and B; βpep28-DOTA; MW 4500.4 Da, Figure 2C and D). Radiolabeling of Ax-DOTA and βpep28-DOTA with ^{111}In resulted in radiochemical yields of greater than 99% (iTLC). Radiochemical purity based on the radio-trace in the analytical HPLC chromatogram was greater than 95%, thus enabling use of the tracer in our *in vitro* and *in vivo* studies without any further purification (Figure 3). In fact, HPLC-derived radiochemical purity values tended to underestimate the real value, as ^{111}In-Ax was partly retained on the column.

In vitro studies. Overexpression of galectin-1 in EC-RF24 cells was stimulated for subsequent cell binding studies with radiolabeled Anginex. In addition, cell-binding experiments were performed with galectin-1-positive (MDA-MD-231-LITG) and galectin-1-negative cancer cell lines (LS174T). Longitudinal *in vitro* binding studies with EC-RF24 cells (Figure 4) showed an exponential increase in ^{111}In-Ax binding with incubation time, until equilibrium was reached

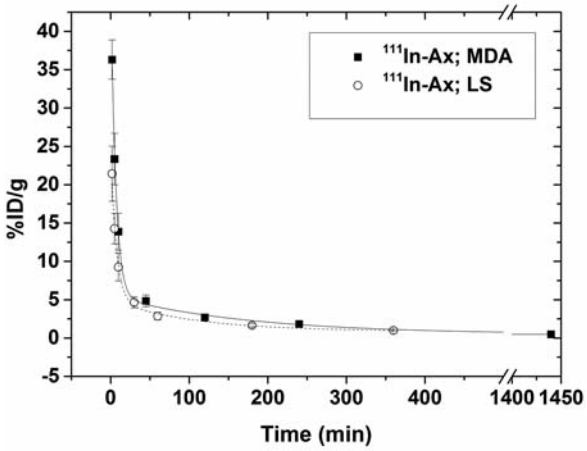

Figure 6. *Blood kinetic profile of ^{111}In-Ax (50 µg/kg b.w.) in MDA-MB-231-LITG (MDA) and LS174T (LS) tumor-bearing mice. Data are presented as %ID/g of tissue±SD (n=3) and fitted with a two-phase exponential decay function.*

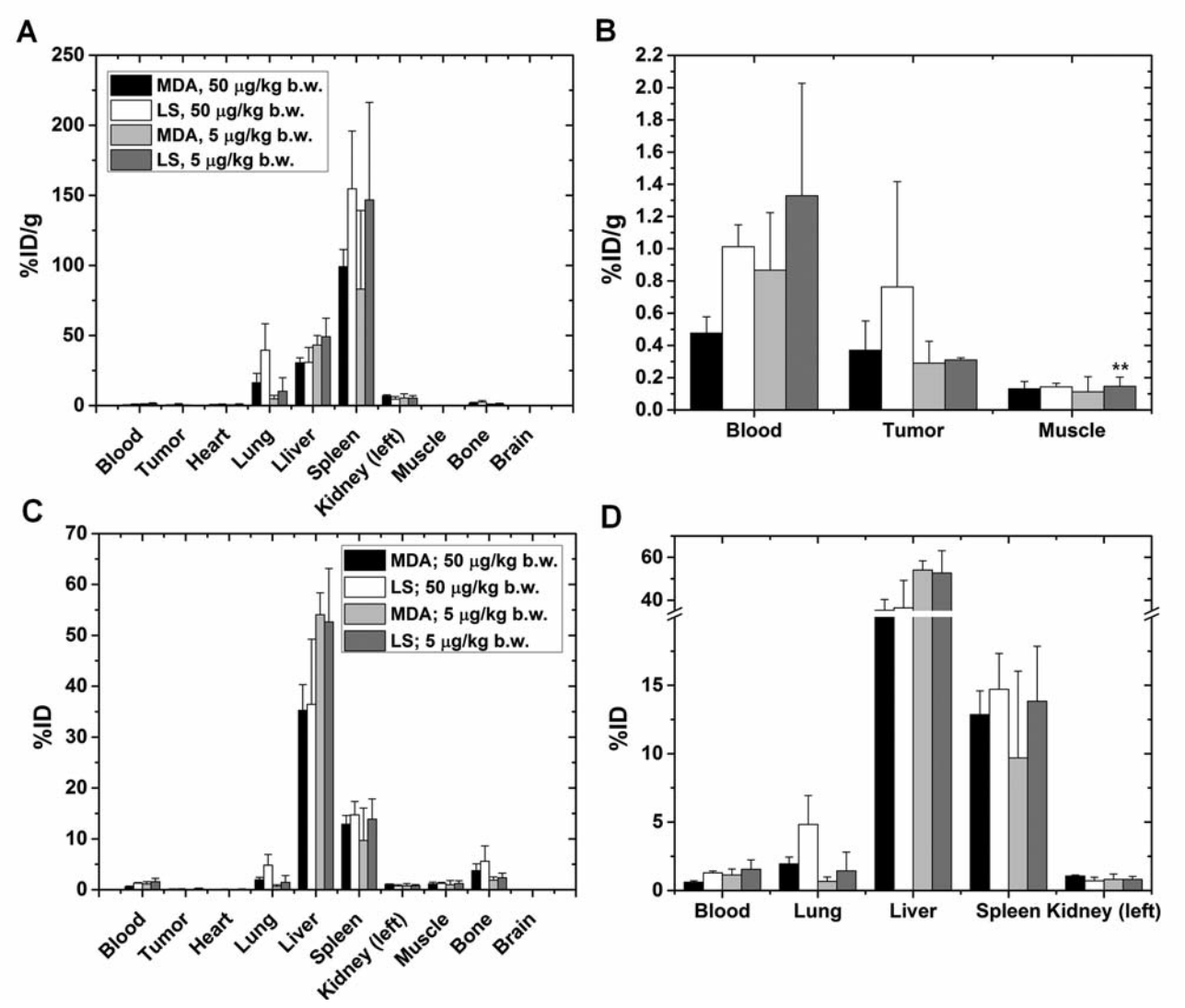

Figure 7. *Biodistribution profiles of ^{111}In-Ax in MDA-MB-231-LITG (MDA) and LS174T (LS) tumor-bearing mice. Data are presented as means±SD (n=3). **p<0.01 vs. tumor uptake.*

after 4 h for experiments performed at both 4˚C and 37˚C. Notably, incubation at 4˚C reduced binding kinetics, as well as the overall extent of binding of ^{111}In-Ax compared to 37˚C (2.5-fold lower binding at t=4 h, $p<0.001$).

Cross-sectional cell binding assays were performed for an incubation time of 4 h to obtain an optimal compromise of tracer accumulation and temperature-dependent cell death at 4˚C. ^{111}In-Ax incubation with galectin-1-expressing EC-RF24 cells at 37˚C (Figure 5A) showed 6.4-fold reduced binding in the presence of excess native Anginex but also a 2.6-fold decrease in the presence of the negative control βpep28 (5.8 *vs.* 0.9 *vs.* 2.2 %ID/μg, respectively, $p<0.001$). A similar trend was observed in binding studies using the galectin-1-positive cell line MDA-MB-231-LITG. Here, incubation with ^{111}In-Ax resulted in a value of 2.2±0.2 %ID/μg, whereas binding was reduced to 0.7±0.1 %ID/μg in the presence of excess native Anginex (3.1-fold lower, $p<0.001$) and to 1.4±0.1 %ID/μg in the presence of βpep28 (1.6-fold lower, $p<0.01$). In contrast to both galectin-1-positive cell lines, the galectin-1-negative cell line LS174T showed negligible binding of ^{111}In-Ax (0.6±0.1 %ID/μg; $p<0.001$ *vs.* EC-RF24 and *vs.* MDA-MB-231-LITG), further evidence that ^{111}In-Ax targets galectin-1. Here, binding of ^{111}In-Ax hardly changed in the presence of an excess of native Anginex or βpep28 (0.4±0.03 %ID/μg and 0.5±0.1 %ID/μg, respectively).

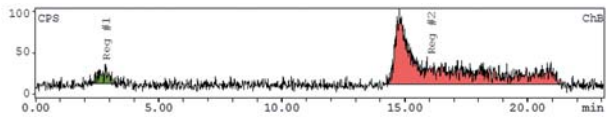

Figure 8. *High-performance liquid chromatography radio-trace of a urine sample containing ^{111}In-Ax 6 h post injection, showing free $^{111}InCl_3$ (Reg #1, 6.36%) and ^{111}In-labeled Anginex (^{111}In-Ax, Reg #2, 93.64%).*

Binding studies with ^{111}In-Ax at 4˚C (Figure 5B) showed an evident decrease when compared to EC-RF24 binding at 37˚C (2.1±0.4 *vs*. 5.8±1.9% ID/μg, respectively). While co-incubation with native Anginex at 4˚C showed a further reduction of binding (2.1-fold, $p<0.001$), competition experiments with βpep28 do not indicate significantly reduced binding of ^{111}In-Ax (2.1±0.4 *vs*. 1.7±0.9 %ID/μg). Even though ^{111}In-Ax binding to MDA-MB-231-LITG or LS174T cells showed a significant decrease when compared to the tracer retention by EC-RF24 cells, no significant differences were obtained within both tumor cell lines when ^{111}In-Ax was co-incubated with native Anginex or βpep28. Furthermore, the ^{111}In-labeled, negative control βpep28 (^{111}In-βpep28) showed negligible retention in all different cell lines at both incubation temperatures (0.003-0.11 %ID/μg).

In vivo blood kinetics and ex vivo biodistribution. In vivo studies were conducted in MDA-MB-231-LITG and LS174T tumor-bearing nude mice injected with ^{111}In-Ax (50 μg/kg b.w.). In both xenograft models, blood kinetic measurements displayed a comparable bi-phasic elimination profile of ^{111}In-Ax (Figure 6). The galectin-1-positive MDA-MB-231-LITG tumor-bearing mice showed a fast initial distribution from the central compartment to the entire body with an α-clearance half-life of $t_{1/2,\alpha}$=3.8±0.2 min (amplitude= 41.0±1.2 %ID/g) and a prolonged elimination phase with a β-half-life of $t_{1/2,\beta}$=44.3±5.2 min (amplitude=6.4±0.4 %ID/g). Half-lives in the galectin-1-negative LS174T tumor-bearing mice were comparable with $t_{1/2,\alpha}$=4.4±1.1 min (amplitude=21.0±3.6 %ID/g) and $t_{1/2,\beta}$=57.1±12.4 min (amplitude=4.6±0.8 %ID/g). The calculated volumes of distribution (V_D) for ^{111}In-Ax were 0.2±0.03 and 0.1±0.01 l/kg in the MDA-MB-231-LITG (C_0=49.2±1.7 %ID/g) and LS174T (C_0=29.5±5.6 %ID/g) tumor model, respectively.

Next, biodistribution experiments were performed to assess the tumor-targeting properties of ^{111}In-Ax (Figure 7). Bolus injections of different doses of ^{111}In-Ax (50 and 5 μg/kg b.w.) resulted in only low uptake in both the galectin-1-positive MDA-MB-231-LITG tumors (0.37±0.18 and 0.29±0.14 %ID/g, respectively) and the negative control LS174T tumors (0.76±0.65 and 0.31±0.01 %ID/g). No significant differences were obtained when comparing tumor-to-blood or tumor-to-muscle ratios between the two tumor models or the two ^{111}In-Ax concentrations. Conversely, for both xenograft models and both tracer doses, high uptake was observed in the lung (6.2-40 %ID/g), liver (31-49 %ID/g), and spleen (99-155 %ID/g). This uptake appeared to be independent of the xenograft model, while higher tracer doses tend to result in lower liver uptake at the expense of a higher lung uptake. Taking organ weights into account, the major excretion occurred *via* liver (35-54 %ID) and spleen (9.7-15 %ID) (Figure 7C and D). Finally, no degradation of the tracer was observed in *ex vivo* urine samples 6 h post-tracer injection (Figure 8).

Discussion

The aim of the present study was to develop the galectin-1-targeting peptide Anginex into a molecular imaging tracer for non-invasive nuclear imaging of tumor angiogenesis and to visualize the *in vivo* behavior of the therapeutic peptide Anginex. To that end, Anginex was modified with a DOTA chelate, which allows radiolabeling with ^{111}In for SPECT imaging. In our study, the peptide βpep28, which is sequentially and structurally homologous to Anginex yet binds galectin-1 with significantly lower affinity, was used as a negative control. We performed *in vitro* binding assays with ^{111}In-Ax and ^{111}In-βpep28 on activated ECs to mimic ECs found in angiogenic blood vessels, as well as on galectin-1 overexpressing tumor cells (MDA-MB-231-LITG) and galectin-1-negative cells (LS174T) (28). Competition assays with Anginex and βpep28 were performed to assess the specificity of the binding of the ^{111}In-labeled tracer for targeting of galectin-1. For *in vitro* studies, binding of ^{111}In-Ax was expected to correlate with overexpression of galectin-1 on the cell surface. For the *in vivo* experiments however, tracer uptake was expected to be comparable for galectin-1-positive (MDA-MB-231-LITG) and galectin-1-negative (LS174T) tumors, because both tumor types should have similar angiogenic vessels with galectin-1-overexpressing ECs (28). Although an elevated tracer uptake in MDA-MB-231-LITG tumors could occur due to endothelial uptake of tumor-derived galectin-1, large variations were not expected (15). Incubation of EC-RF24 cells with ^{111}In-Ax at 37˚C showed uptake that increased exponentially with time, reaching a maximum after 4 h incubation. Assays performed at 4˚C showed strongly reduced uptake of ^{111}In-Ax, which is most likely due to reduced cellular internalization at low temperatures. These results are in agreement with the assumption that galectin-1 acts as an internalizing receptor (15). Competition assays at 37˚C resulted in a 6.4-fold reduction in binding of ^{111}In-Ax to galectin-1. Tracer uptake was also observed in the galectin-1-positive breast cancer cell

line MDA-MB-231-LITG, although it was less compared to to with activated EC-RF24 cells. Again, competition assays with Anginex showed reduced cellular uptake of ^{111}In-Ax. As expected, minimal uptake of ^{111}In-Ax was observed in the galectin-1-negative cell line LS174T (9.7-fold lower as compared to activated ECs). These results therefore demonstrate the specific binding of ^{111}In-Ax to galectin-1. However, competition assays with the negative control βpep28 at 37˚C also resulted in a 2.6-fold lowered binding to the activated ECs ($p<0.01$). As βpep28 was used as a negative control to Anginex, reduced uptake of the ^{111}In-Ax tracer was not expected in the competition experiments (17). Interestingly, in the binding studies conducted at 4˚C, uptake of ^{111}In-Ax dropped almost 3-fold compared to the experiment at 37˚C, while in the competition assays in the presence of βpep28, uptake remained mostly unaltered. This may suggest that βpep28 does not interfere with binding of ^{111}In-Ax to galectin-1, but instead the comparably high dose of βpep28 may to some degree inhibit internalization of ^{111}In-Ax through different, yet unknown mechanisms. This hypothesis is also supported by our finding that incubation assays with radiolabeled βpep28-DOTA displayed minimal retention to galectin-1-expressing cells.

Next, we evaluated behavior of ^{111}In-Ax *in vivo*. The tracer showed a fast distribution across the body post injection which is typical for small compounds such as peptides. Calculated volumes of distribution (V_D=0.1-0.2 l/kg) suggest a rapid distribution of the tracer throughout the extravascular and extracellular space without any significant crossing of cell membranes (29). However, biodistribution studies showed neither tumor-specific uptake of ^{111}In-Ax nor any significant difference in tumor uptake between galectin-1-positive and -negative tumor models. Furthermore, no dose-escalation effect was observed as the tumor-to-blood or tumor-to-muscle ratios in the different groups (injected amount of ^{111}In-Ax: 50 *vs*. 5 μg/kg b.w.) were comparable within statistically significant limits. For both doses, a high uptake of ^{111}In-Ax in non-target organs, such as the kidneys, lung, liver and spleen, was observed. Renal clearance was expected because a strong kidney accumulation is typical for relatively small peptides such as Anginex (30). The large uptake in liver and spleen is most likely caused by the hydrophobic nature and the positive charge of the peptide. Based on *in vivo* observations, the tracer may form aggregates leading to an elevated lung uptake, as well as liver and spleen uptake *via* macrophages, due to the hydrophobic nature of the peptide. Its positive charge could also contribute to greater liver and spleen uptakes and has been observed in other studies with positively charged peptides (31-33).

Our promising *in vitro* findings are in line with earlier studies of Brandwijk and Kluza, who obtained similar *in vitro* results (23, 24). Brandwijk *et al*. prepared fluorescently labeled paramagnetic liposomal formulations modified with Anginex as a targeting moiety on the exterior and showed enhanced uptake of the modified liposomes in activated ECs (23). This binding was diminished in competition assays, demonstrating the potential of these Anginex-conjugated paramagnetic liposomes for MRI of activated ECs *in vitro*. In follow-up studies, Kluza and co-workers functionalized nanoparticles with both Anginex and the $a_v\beta_3$ integrin binding ligand RGD, hereby investigating the utility of dual-targeted liposomes as compared to single-ligand targeting (24, 25). They showed a significant increase in liposomal uptake in activated ECs of simultaneously targeted nanoparticles in comparison to single targeting, as well as a synergistic effect in the dual-targeting strategy. As the Anginex peptide is positively charged (+5.1 net charge at pH 7.0), it is quite likely that these liposomes carrying multiple Anginex molecules have an overall positive net charge and can be considered cationic nanoparticles. As the cell surface charge is negative, a charge-driven interaction next to the ligand-receptor interaction could have had an additional contribution similar to that of positively charged cationic transfection agents or cationic cell penetrating peptides. The latter are known to be reliant on charge-mediated uptake *via* energy-independent uptake pathways (direct translocation *via* pore formation) and various endocytotic pathways, such as macropinocytosis and caveolae-mediated uptake (34-36).

In vivo, Apana *et al*. visualized a BN myeloma tumor/bone graft using [^{18}F]fluorobenzaldehyde labeled Anginex (^{18}F-FBA-Ax) (37). The tumor-to-muscle ratio was in the range of 2.5-5, which is comparable to the maximum ratio of 5.3 observed in our study with ^{111}In-Ax (50 μg/kg b.w.) for LS174T tumor-bearing mice. However, since a relatively large amount of tracer was still present in the blood stream (0.5-1.3 %ID/g in our study, tumor-to-blood ratio of 0.2-0.8), the elevated tumor-to-muscle ratio could well have been caused by a substantial blood content in the tumor due to strong tumor vascularization. Furthermore, information on injected tracer concentration, injection volume or a full biodistribution of ^{18}F-FBA-Ax was not provided in this study, which makes direct comparison of the two tracers impossible. Recently, calixarene-based topomimetics of Anginex were developed for therapeutic purposes. These small organic compounds were shown to display improved anti-angiogenic and anti-tumoral properties over Anginex [calculated half maximal inhibitory concentration (IC_{50}) Anginex=5 μM; topomimetic 0118=2 μM; 0118 analog=0.5 μM] (38-42). However, although topomimetic 0118 and analogs thereof hold promise as therapeutic agents, they may not be suitable for development as molecular imaging tracers (42). Thus, the search for other, more potent high-affinity ligands for the vital angiogenesis target galectin-1 will remain a focus of future research endeavors.

In conclusion, ^{111}In-Ax selectively targets galectin-1 *in vitro* when galectin-1 is overexpressed on cell lines such as EC-RF24 and MDA-MB-231-LITG. Reduced binding of the

tracer in competition assays with native Anginex strongly suggests selective binding to galectin-1, although non-specific binding to the outer leaflet of the plasma membrane due to charge interaction cannot be excluded. While these *in vitro* results are promising, so far the *in vivo* experiments have not shown sufficient tumor targeting of ^{111}In-Ax but a high uptake of the tracer in non-target organs. We therefore conclude that although the anti-angiogenic peptide Anginex is a viable therapeutic compound, the tracer in its current form is not suitable for further development as a tracer for molecular imaging of tumor angiogenesis.

Acknowledgements

The Authors would like to thank Monique Berben (Philips Research), Caren van Kammen, Carlijn van Helvert, Melanie Blonk, and Marije Janssen (Maastricht University) for their support in experiments. This research was performed within the framework of the Center for Translational Molecular Medicine (CTMM), project Mammoth (grant 03O-201).

References

1 Hanahan D and Weinberg RA: The hallmarks of cancer. Cell *100(1)*: 57-70, 2000.
2 Hanahan D and Weinberg RA: Hallmarks of cancer: the next generation. Cell *144(5)*: 646-674, 2011.
3 Carmeliet P and Jain RK: Angiogenesis in cancer and other diseases. Nature *407(6801)*: 249-257, 2000.
4 Folkman J: Angiogenesis in cancer, vascular, rheumatoid and other disease. Nat Med *1(1)*: 27-31, 1995.
5 Cao Y and Langer R: A review of Judah Folkman's remarkable achievements in biomedicine. Proc Natl Acad Sci USA *105(36)*: 13203-13205, 2008.
6 Folkman J: Tumor angiogenesis: therapeutic implications. N Engl J Med *285(21)*: 1182-1186, 1971.
7 Griffioen AW and Molema G: Angiogenesis: potentials for pharmacologic intervention in the treatment of cancer, cardiovascular diseases, and chronic inflammation. Pharmacol Rev *52(2)*: 237-268, 2000.
8 Weissleder R and Pittet MJ: Imaging in the era of molecular oncology. Nature *452(7187)*: 580-589, 2008.
9 Potente M, Gerhardt H and Carmeliet P: Basic and therapeutic aspects of angiogenesis. Cell 146(6): 873-887, 2011.
10 Neri D and Bicknell R: Tumour vascular targeting. Nat Rev Cancer *5(6)*: 436-446, 2005.
11 Thijssen VL, Postel R, Brandwijk RJ, Dings RP, Nesmelova I, Satijn S, Verhofstad N, Nakabeppu Y, Baum LG, Bakkers J, Mayo KH, Poirier F and Griffioen AW: Galectin-1 is essential in tumor angiogenesis and is a target for antiangiogenesis therapy. Proc Natl Acad Sci USA *103(43)*: 15975-15980, 2006.
12 Ito K, Stannard K, Gabutero E, Clark AM, Neo SY, Onturk S, Blanchard H and Ralph SJ: Galectin-1 as a potent target for cancer therapy: role in the tumor microenvironment. Cancer Metastasis Rev *31(3-4)*: 763-778, 2012.
13 Thijssen VL, Poirier F, Baum LG and Griffioen AW: Galectins in the tumor endothelium: opportunities for combined cancer therapy. Blood *110(8)*: 2819-2827, 2007.
14 Thijssen VL, Hulsmans S and Griffioen AW: The galectin profile of the endothelium: altered expression and localization in activated and tumor endothelial cells. Am J Pathol *172(2)*: 545-553, 2008.
15 Thijssen VL, Barkan B, Shoji H, Aries IM, Mathieu V, Deltour L, Hackeng TM, Kiss R, Kloog Y, Poirier F and Griffioen AW: Tumor cells secrete galectin-1 to enhance endothelial cell activity. Cancer Res *70(15)*: 6216-6224, 2010.
16 Carlsson MC, Cederfur C, Schaar V, Balog CI, Lepur A, Touret F, Salomonsson E, Deelder AM, Ferno M, Olsson H, Wuhrer M and Leffler H: Galectin-1-binding glycoforms of haptoglobin with altered intracellular trafficking, and increase in metastatic breast cancer patients. PLoS One *6(10)*: e26560, 2011.
17 Griffioen AW, van der Schaft DW, Barendsz-Janson AF, Cox A, Struijker Boudier HA, Hillen HF and Mayo KH: Anginex, a designed peptide that inhibits angiogenesis. Biochem J *354(Pt 2)*: 233-242, 2001.
18 van der Schaft DW, Dings RP, de Lussanet QG, van Eijk LI, Nap AW, Beets-Tan RG, Bouma-Ter Steege JC, Wagstaff J, Mayo KH and Griffioen AW: The designer anti-angiogenic peptide anginex targets tumor endothelial cells and inhibits tumor growth in animal models. Faseb J *16(14)*: 1991-1993, 2002.
19 Dings RP, van der Schaft DW, Hargittai B, Haseman J, Griffioen AW and Mayo KH: Anti-tumor activity of the novel angiogenesis inhibitor anginex. Cancer Lett *194(1)*: 55-66, 2003.
20 Arroyo MM and Mayo KH: NMR solution structure of the angiostatic peptide anginex. Biochim Biophys Acta *1774(5)*: 645-651, 2007.
21 Ilyina E, Roongta V and Mayo KH: NMR structure of a *de novo* designed, peptide 33mer with two distinct, compact beta-sheet folds. Biochemistry *36(17)*: 5245-5250, 1997.
22 Wang JB, Wang MD, Li EX and Dong DF: Advances and prospects of anginex as a promising anti-angiogenesis and anti-tumor agent. Peptides *38(2)*: 457-462, 2012.
23 Brandwijk RJ, Mulder WJ, Nicolay K, Mayo KH, Thijssen VL and Griffioen AW: Anginex-conjugated liposomes for targeting of angiogenic endothelial cells. Bioconjug Chem *18(3)*: 785-790, 2007.
24 Kluza E, van der Schaft DW, Hautvast PA, Mulder WJ, Mayo KH, Griffioen AW, Strijkers GJ and Nicolay K: Synergistic targeting of alphavbeta3 integrin and galectin-1 with heteromultivalent paramagnetic liposomes for combined MR imaging and treatment of angiogenesis. Nano Lett *10(1)*: 52-58, 2010.
25 Kluza E, Jacobs I, Hectors SJ, Mayo KH, Griffioen AW, Strijkers GJ and Nicolay K: Dual-targeting of alphavbeta3 and galectin-1 improves the specificity of paramagnetic/fluorescent liposomes to tumor endothelium *in vivo*. J Control Release *158(2)*: 207-214, 2012.
26 Apana MA, Griffin RJ, Koonce NA, Webber JS, Dings RPM, Mayo KH and Berridge MS: Synthesis of [^{18}F]anginex with high specific activity [^{18}F]fluorobenzaldehyde for targeting angiogenic activity in solid tumors. J Label Compd Radiopharm *54(11)*: 708-713, 2011.
27 van Beijnum JR, van der Linden E and Griffioen AW: Angiogenic profiling and comparison of immortalized endothelial cells for functional genomics. Exp Cell Res *314(2)*: 264-272, 2008.
28 Lahm H, Andre S, Hoeflich A, Fischer JR, Sordat B, Kaltner H, Wolf E and Gabius HJ: Comprehensive galectin fingerprinting

in a panel of 61 human tumor cell lines by RT-PCR and its implications for diagnostic and therapeutic procedures. J Cancer Res Clin Oncol *127(6)*: 375-386, 2001.

29 Smith DA, Van de Waterbeemd H and Walker DK: Pharmacokinetics and Metabolism in Drug Design. 2nd edn.Wiley-VCH Verlag GmbH: Weinheim, 2001.

30 Wynendaele E, Bracke N, Stalmans S and De Spiegeleer B: Development of peptide and protein based radiopharmaceuticals. Curr Pharm Des *20(14)*: 2250-2267, 2014.

31 van Duijnhoven SM, Robillard MS, Nicolay K and Grull H: Tumor targeting of MMP-2/9 activatable cell-penetrating imaging probes is caused by tumor-independent activation. J Nucl Med *52(2)*: 279-286, 2011.

32 Jarver P, Mager I and Langel U: In vivo biodistribution and efficacy of peptide mediated delivery. Trends Pharmacol Sci *31(11)*: 528-535, 2010.

33 Seo J, Ren G, Liu H, Miao Z, Park M, Wang Y, Miller TM, Barron AE and Cheng Z: In vivo biodistribution and small animal PET of (64)Cu-labeled antimicrobial peptoids. Bioconjug Chem *23(5)*: 1069-1079, 2012.

34 Frohlich E: The role of surface charge in cellular uptake and cytotoxicity of medical nanoparticles. Int J Nanomedicine *7*: 5577-5591, 2012.

35 Farkhani SM, Valizadeh A, Karami H, Mohammadi S, Sohrabi N and Badrzadeh F: Cell penetrating peptides: efficient vectors for delivery of nanoparticles, nanocarriers, therapeutic and diagnostic molecules. Peptides *57*: 78-94, 2014.

36 Lin J and Alexander-Katz A: Cell membranes open "doors" for cationic nanoparticles/biomolecules: insights into uptake kinetics. ACS Nano *7(12)*: 10799-10808, 2013.

37 Apana SM, Griffin RJ, Koonce NA, Webber JS, Dings RPM, Mayo KH and Berridge MS: Synthesis of [^{18}F]anginex with high specific activity [^{18}F]fluorobenzaldehyde for targeting angiogenic activity in solid tumors. J Label Compd Radiopharm *54(11)*: 708-713, 2011.

38 Dings RP, Chen X, Hellebrekers DM, van Eijk LI, Zhang Y, Hoye TR, Griffioen AW and Mayo KH: Design of nonpeptidic topomimetics of antiangiogenic proteins with antitumor activities. J Natl Cancer Inst *98(13)*: 932-936, 2006.

39 Dings RP, Kumar N, Miller MC, Loren M, Rangwala H, Hoye TR and Mayo KH: Structure-based optimization of angiostatic agent 6DBF7, an allosteric antagonist of galectin-1. J Pharmacol Exp Ther *344(3)*: 589-599, 2013.

40 Dings RP, Miller MC, Nesmelova I, Astorgues-Xerri L, Kumar N, Serova M, Chen X, Raymond E, Hoye TR and Mayo KH: Antitumor agent calixarene 0118 targets human galectin-1 as an allosteric inhibitor of carbohydrate binding. J Med Chem *55(11)*: 5121-5129, 2012.

41 Dings RPM, Laar ESv, Webber J, Zhang Y, Griffin RJ, Waters SJ, MacDonald JR and Mayo KH: Ovarian tumor growth regression using a combination of vascular targeting agents anginex or topomimetic 0118 and the chemotherapeutic irofulven. Cancer Lett *265*: 270-280, 2008.

42 Lappchen T, Dings RP, Rossin R, Simon JF, Visser TJ, Bakker M, Walhe P, van Mourik T, Donato K, van Beijnum JR, Griffioen AW, Lub J, Robillard MS, Mayo KH and Grull H: Novel analogs of antitumor agent calixarene 0118: Synthesis, cytotoxicity, click labeling with 2-[(18)F]fluoroethylazide, and *in vivo* evaluation. Eur J Med Chem *89*: 279-295, 2015.

Received July 14, 2015
Revised September 1, 2015
Accepted September 16, 2015